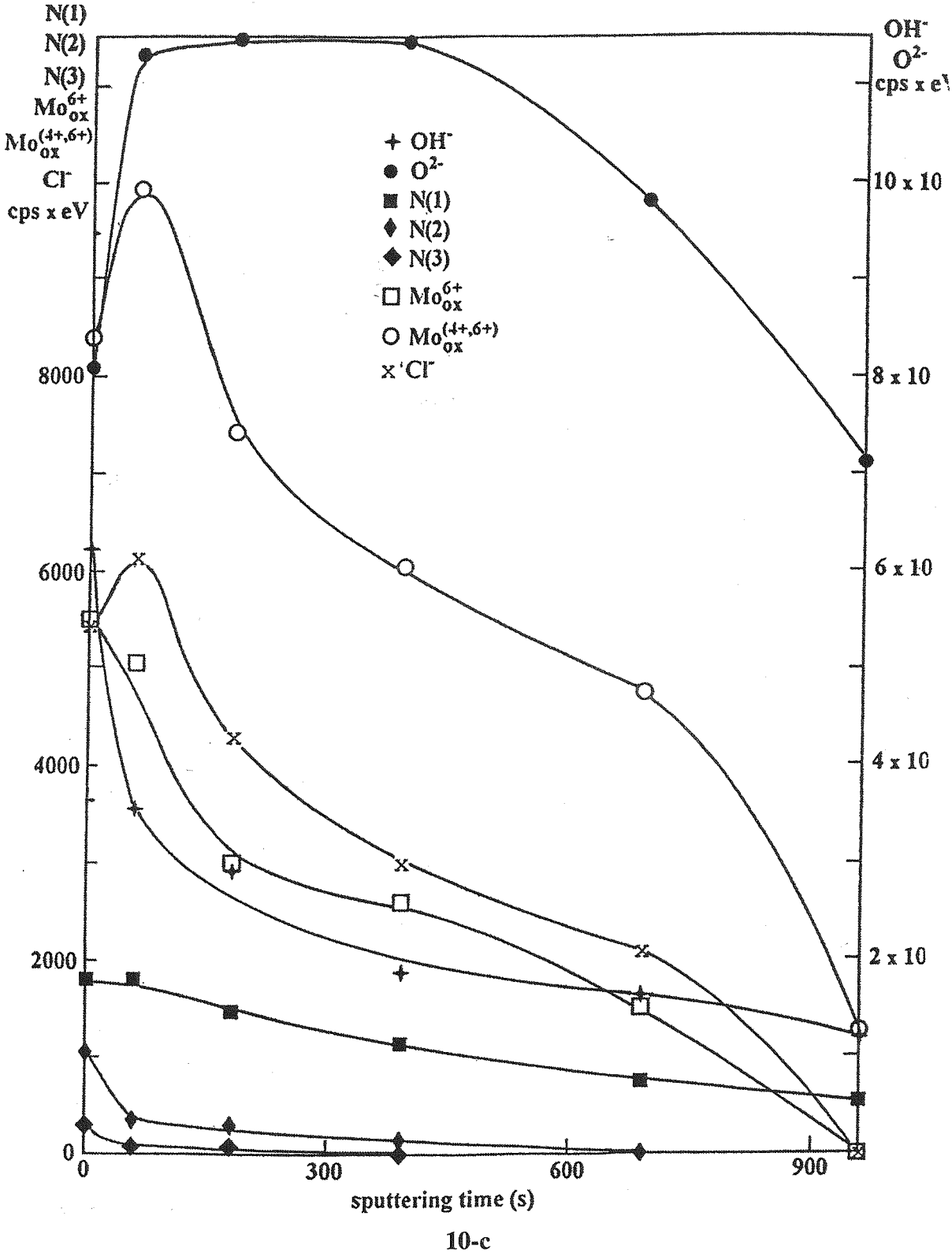

10-c

Figure (10) XPS depth profiles after passivation of the Fe17Cr13Ni3Mo0.07N alloy; 650mV/SHE, 30min a) in 0.5M H_2SO_4 b) in 0.5M H_2SO_4+0.8M NaCl c) in 1.5M NaCl (pH=1.5).

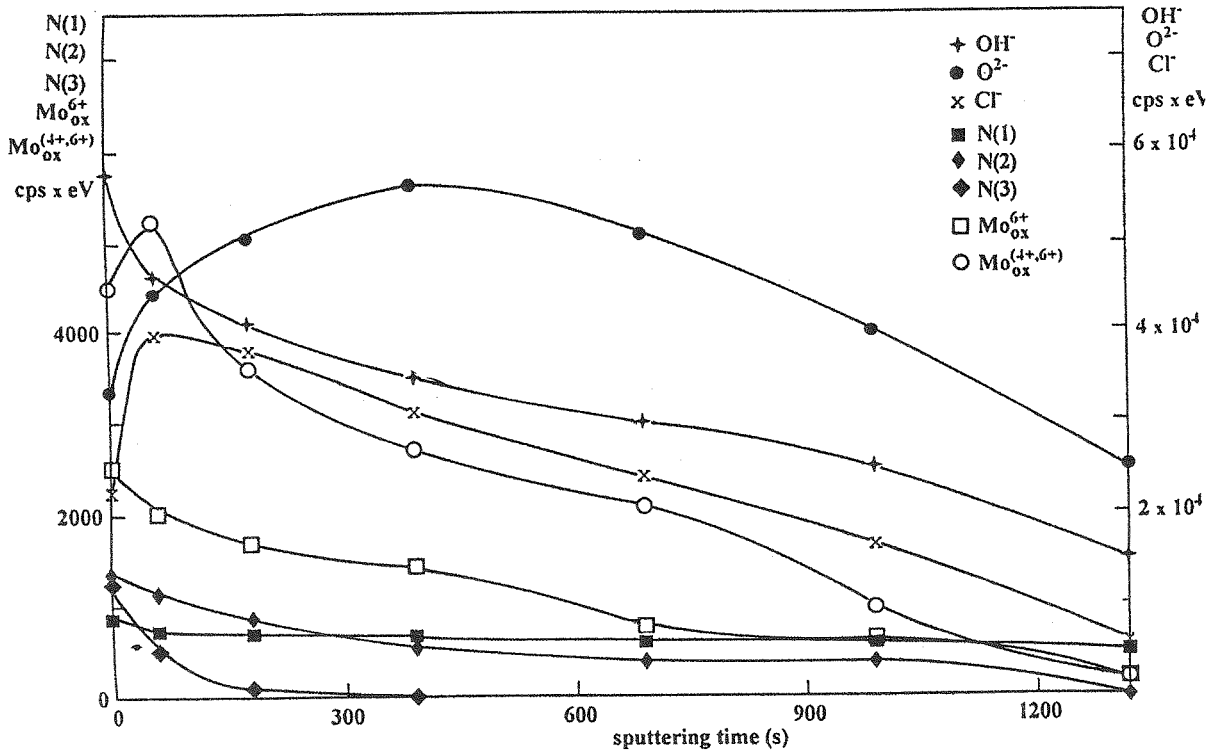
N(1)
N(2)
N(3)
Mo_{ox}^{6+}
$Mo_{ox}^{(4+,6+)}$
cps x eV
4000
2000
0
0
300
600
900
1200
sputtering time (s)
OH⁻
O^{2-}
Cl^-
cps x eV
6×10^{-4}
4×10^{-4}
2×10^{-4}
OH⁻
O^{2-}
Cl^-
N(1)
N(2)
N(3)
Mo_{ox}^{6+}
$Mo_{ox}^{(4+,6+)}$

10-b

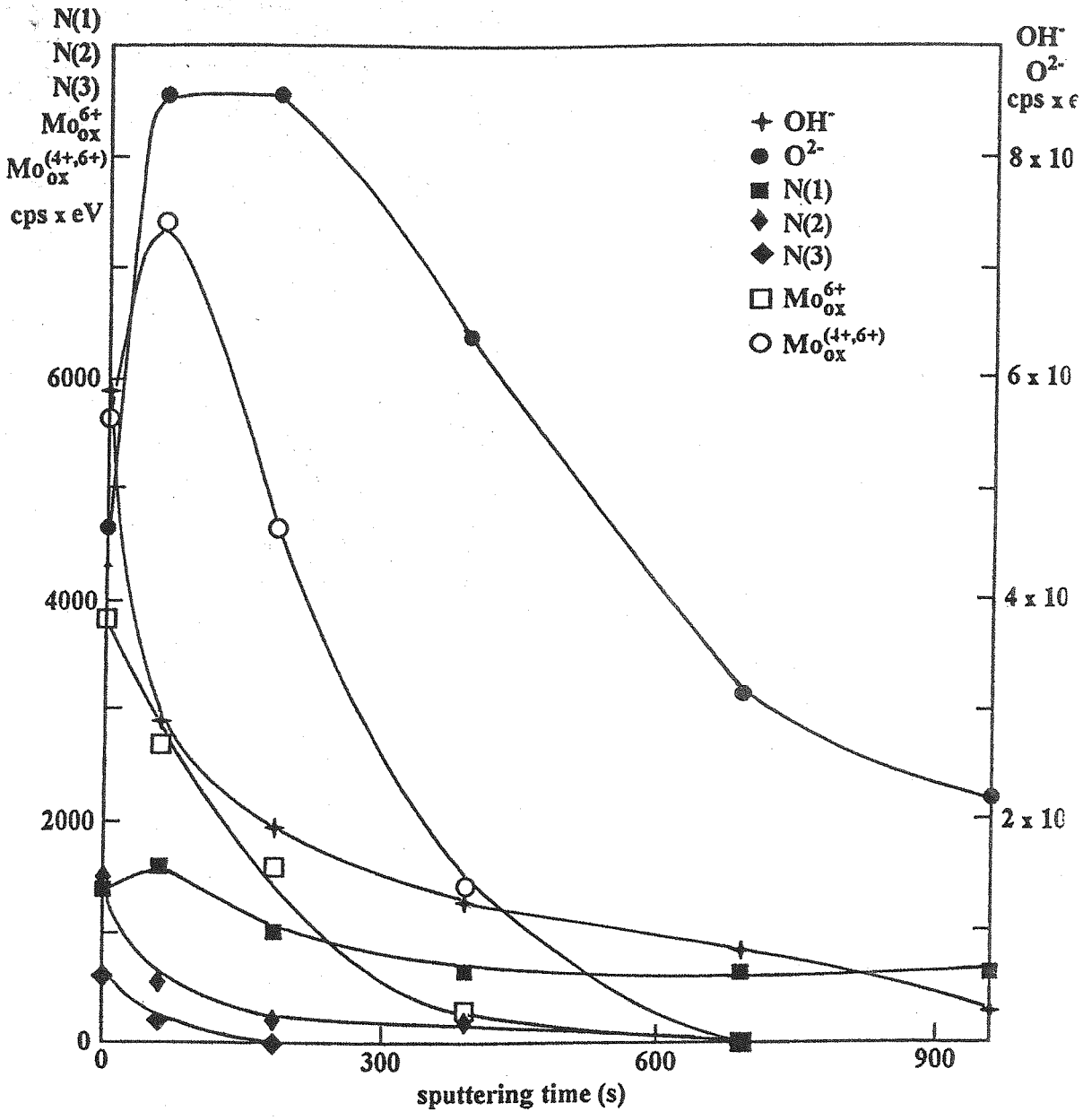
N(1)
N(2)
N(3)
Mo_{ox}^{6+}
$Mo_{ox}^{(4+,6+)}$
cps x eV
6000
4000
2000
0
0
300
600
900
sputtering time (s)
OH^-
O^{2-}
cps x e
8 x 10
6 x 10
4 x 10
2 x 10
OH^-
O^{2-}
N(1)
N(2)
N(3)
Mo_{ox}^{6+}
$Mo_{ox}^{(4+,6+)}$

10-a

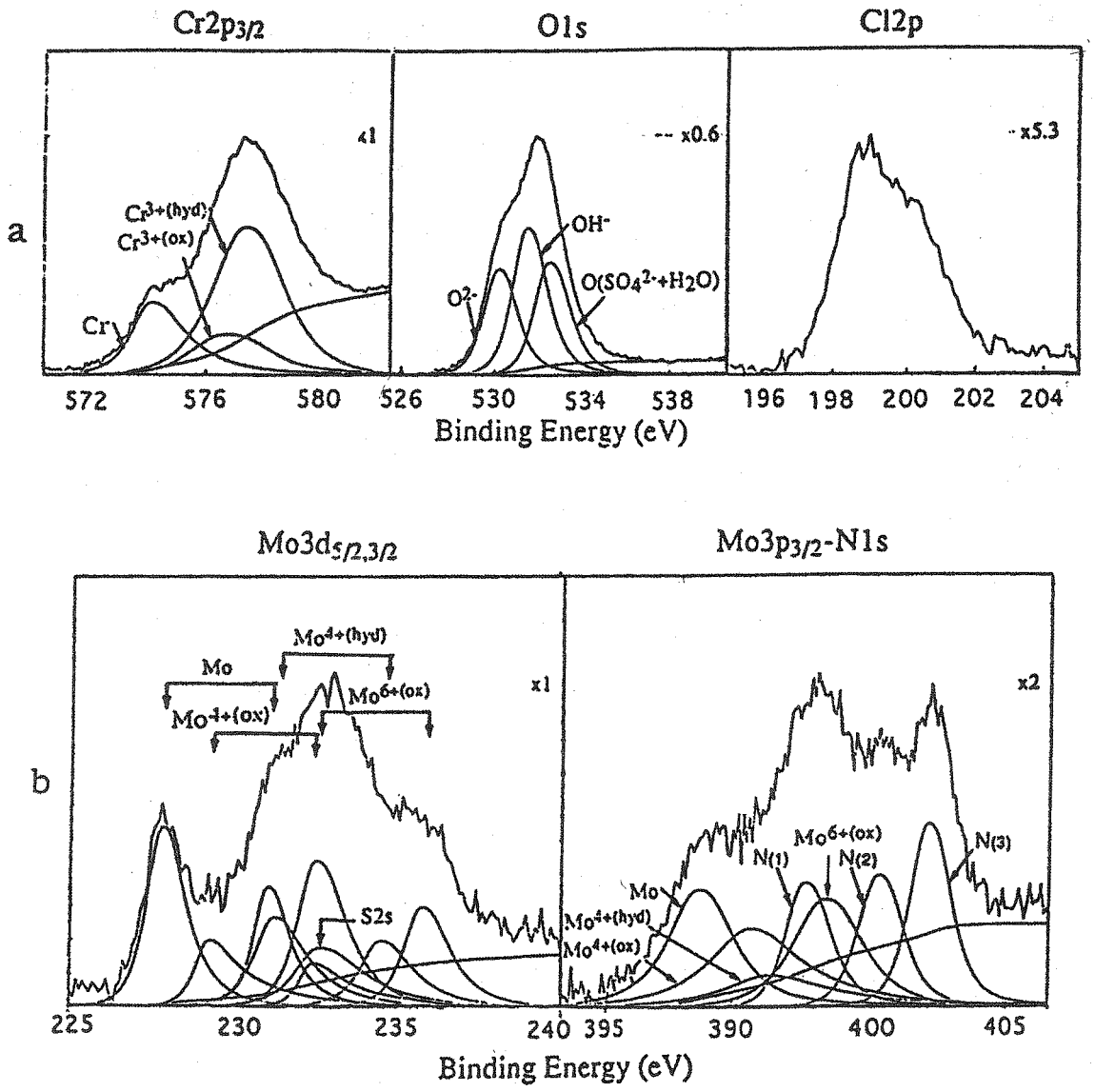

Figure (9) XPS spectra of a) $Cr2p_{3/2}$, Ols and Cl2p and b) $Mo3d_{5/2,3/2}$ and $Mo3p_{3/2}$-Nls after passivation of the Fe17Cr13Ni3Mo0.15N alloy (0.5M H_2SO_4+0.8M NaCl, 650 mV/SHE, 30min).

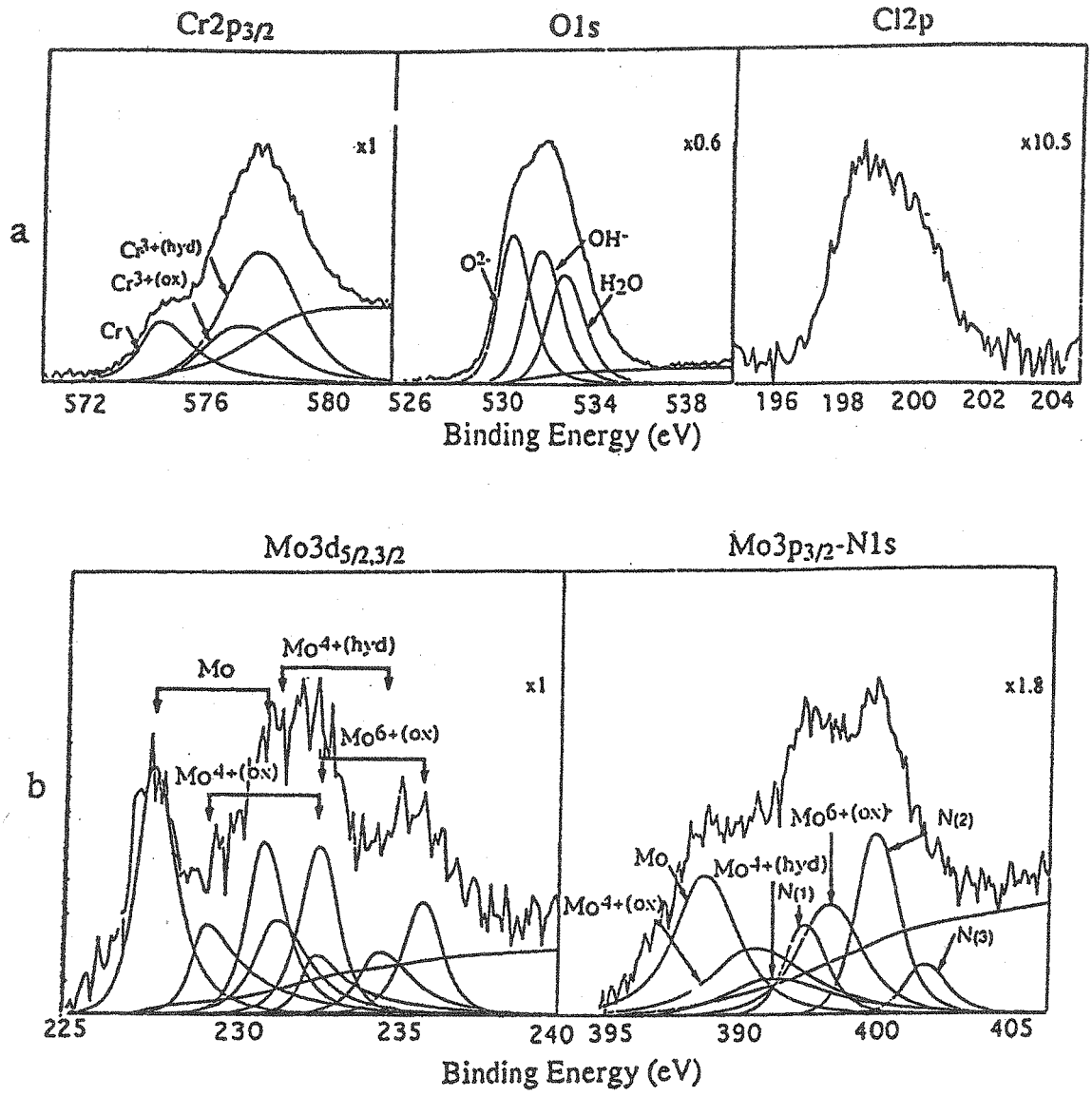

Figure (8) XPS spectra of a) $Cr2p_{3/2}$, Ols and Cl2p and b) $Mo3d_{5/2,3/2}$ and $Mo3p_{3/2}$-Nls of the Fe17Cr13Ni3Mo0.07N alloy after a potentiodynamic sweep from the corrosion potential to 650 mV/SHE (in the passive region): then it was maintained at this potential for 30 minutes in 0.5M H_2SO_4+0.8M NaCl, 650mV/SHE, 30 min. Take off angles: 90°.

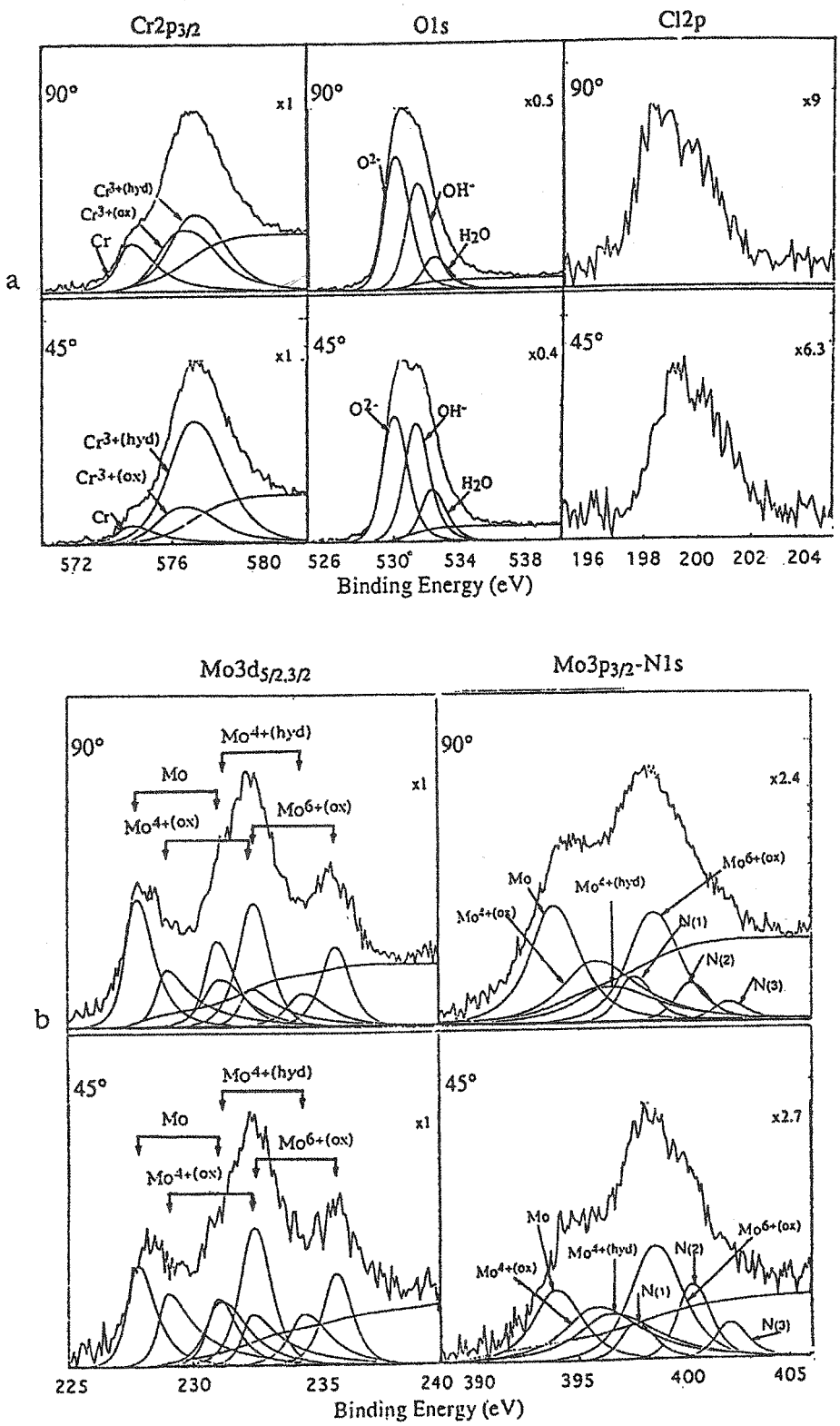

Figure (7) XPS spectra of a) $Cr2p_{3/2}$,Ols and Cl2p and b) $Mo3d_{5/2,3/2}$ and $Mo3p_{3/2}$-Nls after passivation of the Fe17Cr13Ni3Mo0.07N alloy. Take off angles: 90° and 45° (1.5 M NaCl (pH=1.5), 650 mV/SHE, 30min).

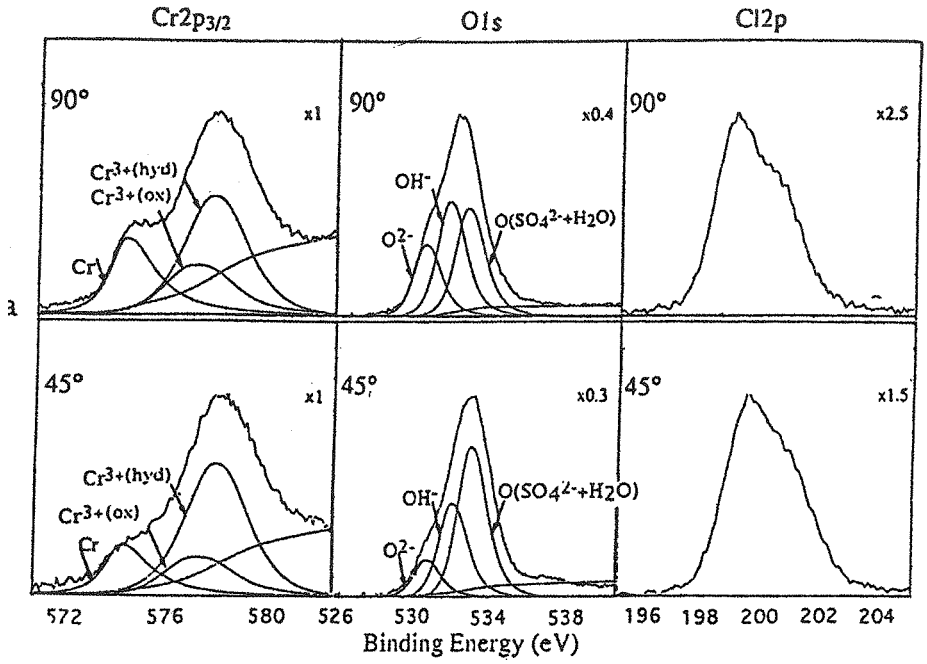

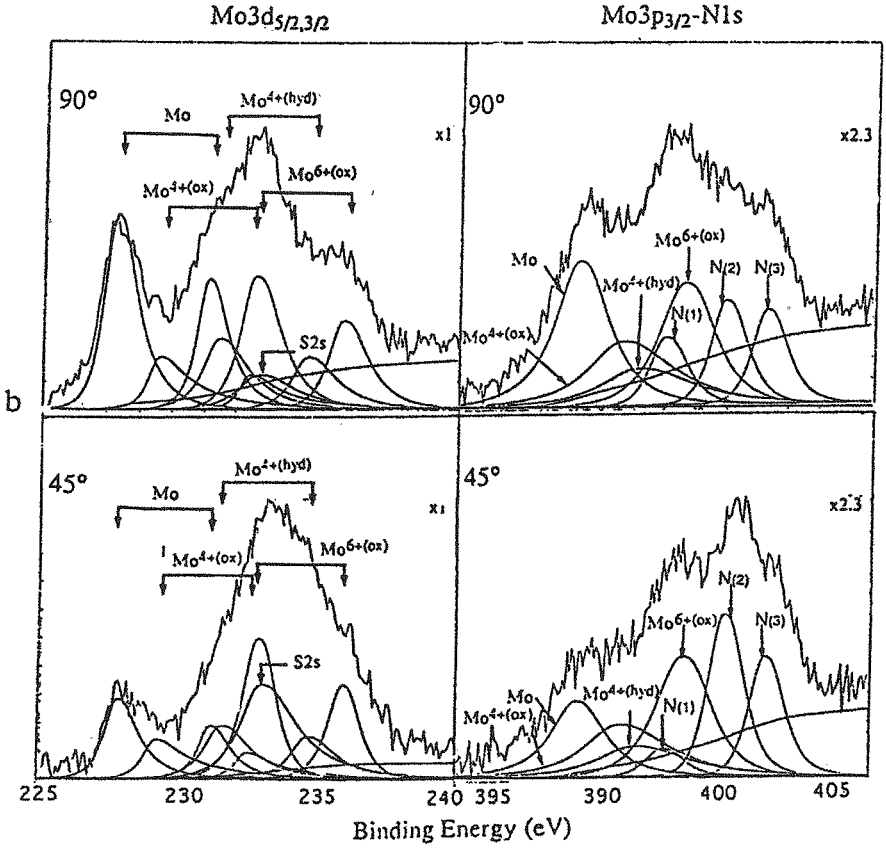

Figure (6) XPS spectra of a) $Cr2p_{3/2}$, Ols and Cl2p and b) $Mo3d_{5/2,3/2}$ and $Mo3p_{3/2}$-Nls after psssivation of the Fe17Cr13Ni3Mo0.07N alloy. Take off angles: 90° and 45° (0.5M H_2SO_4+0.8M NaCl, 650 mV/SHE, 30 min).

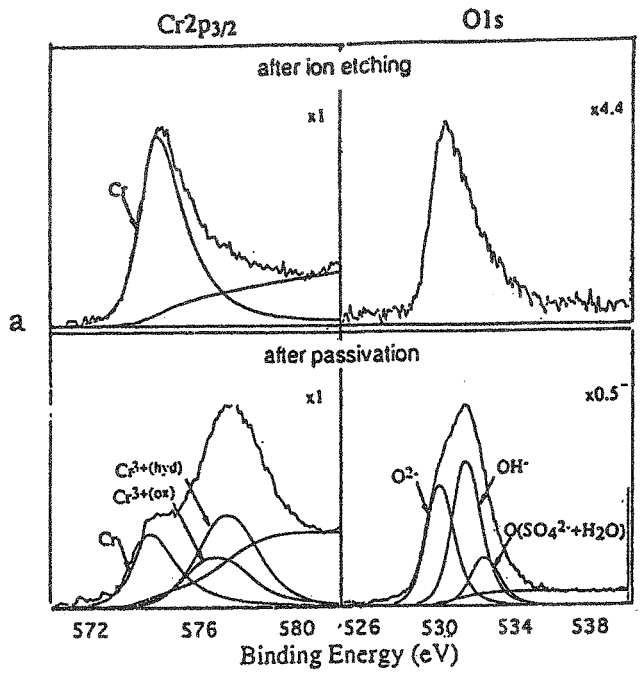

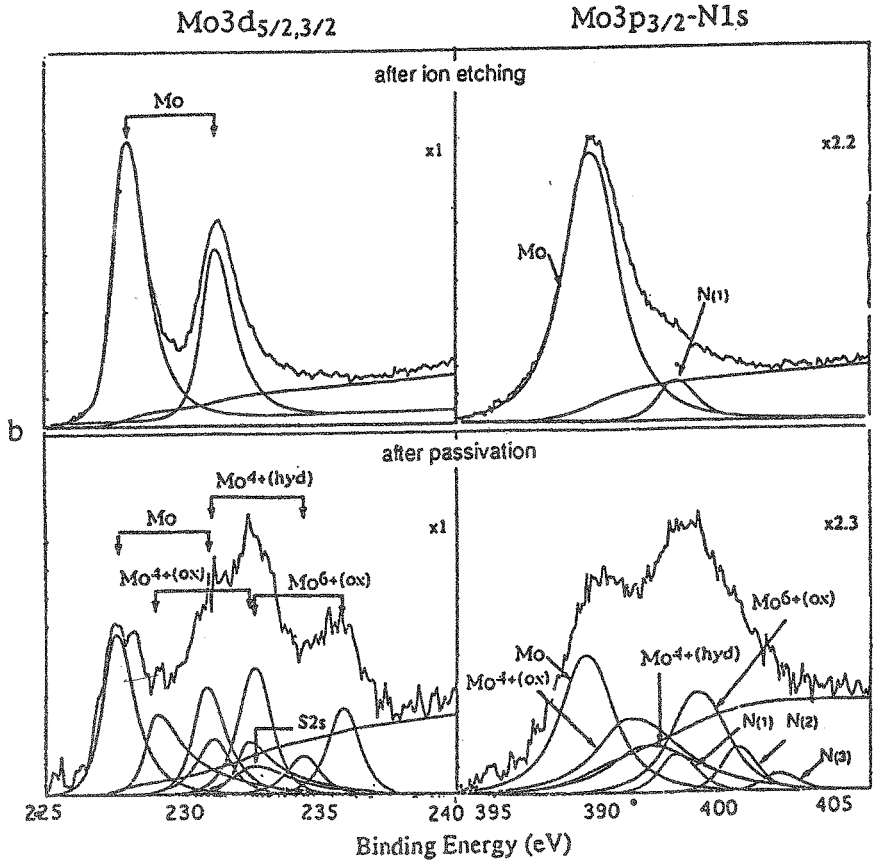

Figure (5) XPS spectra of a) $Cr2p_{3/2}$ and Ols and b) $Mo3d_{5/2,3/2}$ and $Mo3p_{3/2}$-Nls after ion etching and after passivation of the Fe17Cr13Ni3Mo0.07N alloy (0.5M H_2SO_4, 650 mV/SHE, 30min).

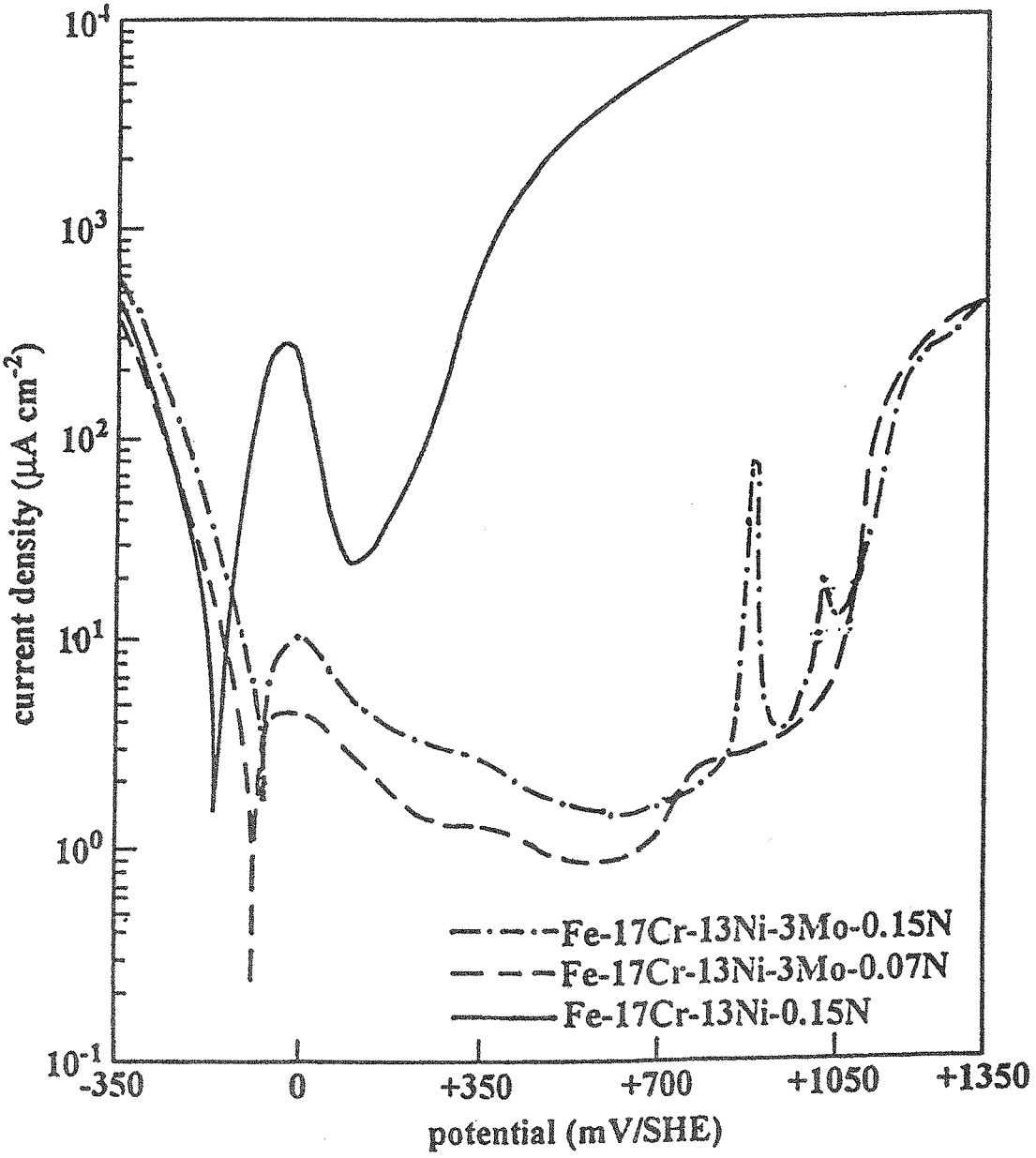

Figure (4) Potentiodynamic curves recorded for the Fe17Cr13Ni3Mo0.15N, Fe17Cr13Ni3Mo0.07N and Fe17Cr13Ni0.15N alloys in 1.5 M NaCl (pH=1.5) (1mV/sec).

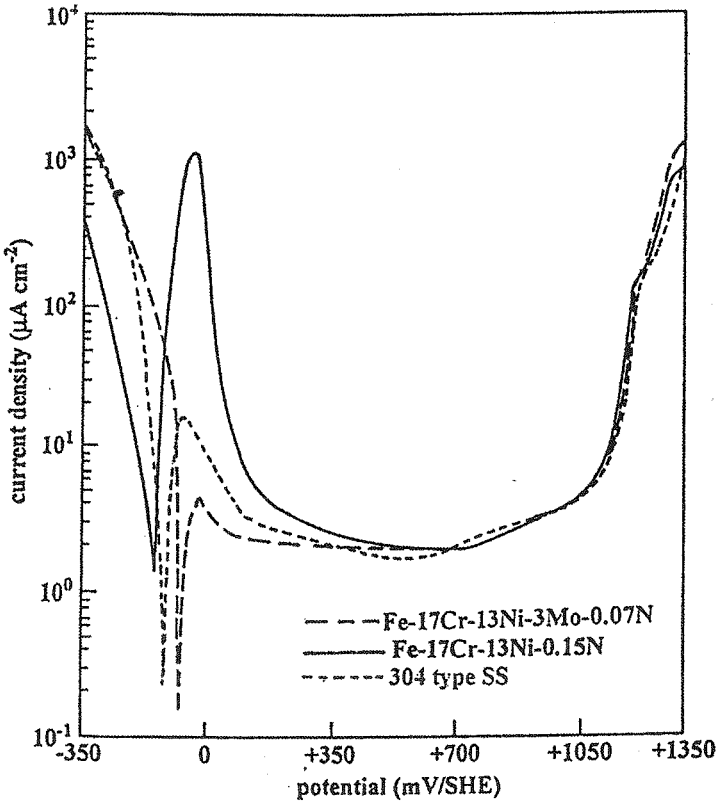

Figure (2) Potentiodynamic curves measured for the Fe17Cr13Ni3Mo0.07N. Fe17Cr13Ni0.15N, and a 304 type stainless steel in 0.5M H_2SO_4 (1mV/sec).

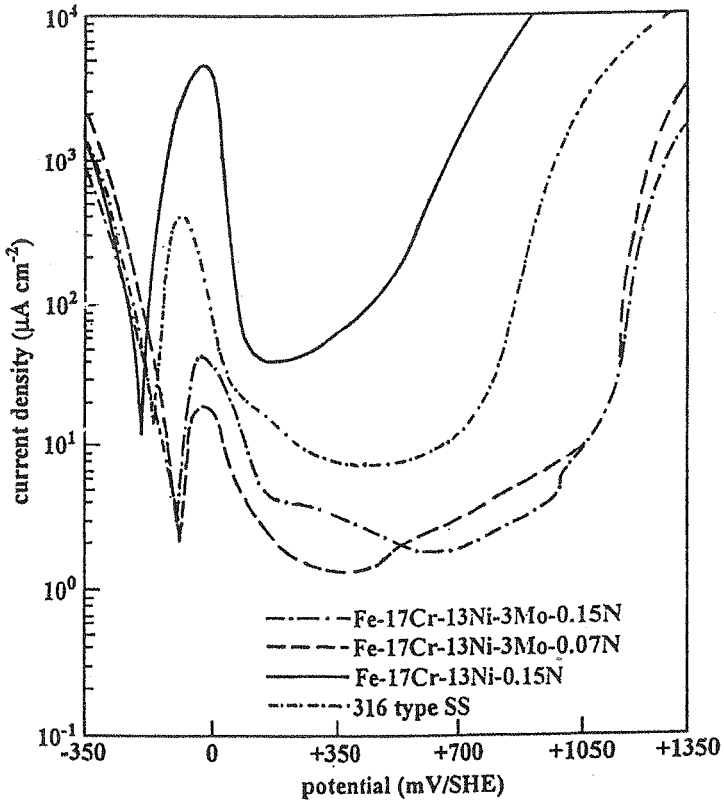

Figure (3) Potentiodynamic curves measurd for the Fe17Cr13Ni3Mo0.15N. Fe17Cr13Ni3Mo0.07N, Fe17Cr13Ni0.15N alloys an a 316 type stainless steel in 0.5M H_2SO_4+0.8 M NaCl (1mV/sec).

References:

1) I. Olefjord, Mat. science and Engineering, 42 (1980): P. 161.
2) I. Olefjord, B. Brox and U. Jelvestam, Electrochem. Soc., 132(1985): P. 2854.
3) C. R. Clayton and Y. C. Lu, J. Electrochemical. Soc., 133 (1986): P. 2465.
4) C. Cohen, D. Schmaus, A. Elbiache and P. Marcus, Corrosion Science, 31 (1990): P. 207.
5) J. E. Castle and J. H. Qiu, Corrosion Science, 30 (1990): P. 429.
6) E. De Vito and P. Marcus Surface Interface Analysis, 19, (1992) 403.
7) Y. C. Lu, R. Bandy C. R. Clayton and R. C. Newman, J. Electrochem. Soc 130, 1774 (1983).
8) J. E. Truman, M. J. Coleman and K. R. Prit. Corros. J. 12, 236 (1977).
9) R. Bandy and D. Van Rooyen, Corros. 39, 227 (1983).
10) J. Eckenrod and C. W. Kovack, ASTM STP 679, p 17 philadelphia, PA (1977).
11) K. Osozawa and N. Okato. Passivity and its Breakdown on Iron and Iron Based Alloys. (USA-Japan Seminar, Honolulu) p 135 Houston, TX NACE (1976).
12) A. Sadough. Vanini and P. Marcus Corrosion Science, 36 (1994): P. 1825.
13) P. Marcus and M. E. Bussell, APPl. Surf. Sci. 59 (1992) 7.
14) Y. C. Lu and C. R. Clayton, Corrosion Science, 29 (1989): p. 927.
15) B. Brox and I. Olefjord, Surf. Interface Anal., 13, 3 (1988).
16) C. R. Clayton, L. Rosensweig, M. Oversluizen and Y. C. Lu, in: surfaces, Inhibition and Passivation, Eds. E. McCafferty and R. J. Brod (Electrochemical Society, Pennington, NJ, (1986) 323.

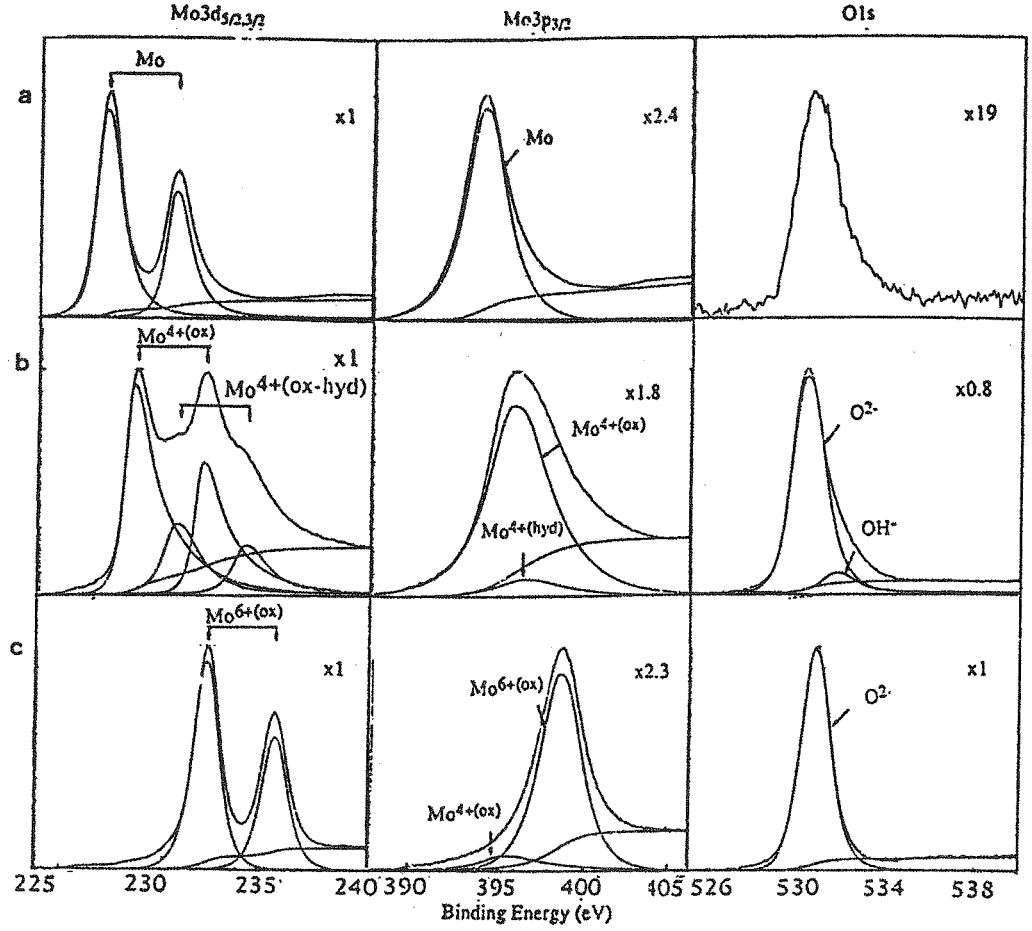

Figure (1) Reference XPS spectra reported with Al KC X-ray source for molybdenum and molybdenum oxides (a) pure Mo (ion-etched) (b) MoO_2 and (c) MoO_3.

creases with sputtering time, confirming that the hydroxide layer constitutes the outer part of the film. The slow decrease of the intensity of the N(1) peak at low binding energy (397.7 eV) corresponding to N-metal bonds, indicates that the nitride is present in the inner part of the passive film near the passive film/alloy interface which confirms the finding of the AD-XPS measurements. The results for N(2) and N(3) at different depths in the passive film show the high binding energy nitrogen species to be mainly at the passive film surface, confirming that it is produced at least in part via reaction with the electrolyte. The sharp decrease of the Mo^{6+} signal observed after the first ion sputtering indicates the Mo^{6+} is located in the outer part of the passive film. The total signal from the oxidized molybdenum ($Mo^{4+,6+}$ in figure 10) decreases rapidly during ion sputtering which also supports the preceding conclusion, even if some reduction of Mo^{6+} may be caused by sputtering. The maior diffrence between the composition depth profiles measured after polarization in 0.5M H_2SO_4 solution and 1.5M NaCl (pH=1.5) solution is the higher surface enrichment of molybdenum oxide (Mo^{6+}, Mo^{4+}) in the 1.5M NaCl (pH=1.5) solution, this confirms the higher dissolution rate and anodic segregation of N(1) in 1.5M NaCl (pH=1.5) solution). The passive film was found to have a bilayer structure both in the absence and in the presence of Cl^- in the stage preceding pitting. The results for the Cl2p XPS spectra at different depths in the passive film show that chlorides are incorporated in the passive film, they are located mostly in the outer part of the film.

Conclusions:

The pitting resistance of the austenitic stainless steels with 3Mo-0.07 N in chloride solution is better than the one of the alloy with 3Mo-0.15N.

Mo and N strongly modify the electrochemical behaviour of the alloy. The dissolution rate is lowered by the Mo in low nitrogen content alloy compared with 3% Mo0.15 %N alloy. In 0.5M H_2SO_4, the active peak is intense in the case of the alloy with 0.15N, lower for the alloy (3Mo-0.15N), and almost suppressed for the (3Mo-0.07N) alloy. The variation of the intensities of the active peak in chloride solution with the composition of the alloy are similar to those in acid media. For the high nitrogen content alloy, the residual current density is higher than for the low nitrogen alloy and pitting-repassivation process is observed at 800mV/SHE (in chloride media, 1.5M NaCl).

The passive film has a bilayer structure and the outer hydroxide layer is enhanced in the chloride-acidic media. Chloride are incorporated in the passive film, they are located mostly in the outer part of the film.

A marked enrichment of the alloyed (Mo) elements is observed in the metallic phase under the passive film and nitrogen enrichment (nitride) is observed in the alloy near the alloy/passive film interface, due to the preferential dissolution of iron. The nitride phase is formed by anodic segregation of the nitrogen contained in the alloy, during the dissolution stage preceding passivation. The rate of anodic segregation of N and Mo enrichement or iron selective dissolution is in the following order: 0.5M H_2SO_4+0.8M NaCl>1.5M NaCl (pH=1.5)>0.5M H_2SO_4. This confirmed by electrochemistry results. The high and intermediate binding energy nitrogen peaks (may originate from N-H or N-O) are assigned to nitrogen species located at the surface of the passive film, and are produced via reaction with the electrolyte, so the intensities of the high binding energy nitrogen peaks depend on the dissolution of the alloy during the dissolution stage preceding passivation.

The oxygen (Ols) region clearly shows the presence of the oxide O^{2-} and hydroxide (OH^-) states. A third peak is present corresponding to oxygen in H_2O and SO_4^{2-}. Oxidized Mo is detected in the analyzed passive film. The Mo signal has been resolved into the metallic form and three oxides states $Mo^{4+(ox)}$ (MoO_2), $Mo^{4+(ox-hyd)}$ $MoO(OH)_2$ type and $Mo^{6+(ox)}$(MoO_3). The curve fitting of the Mo spectrum shows that Mo is mainly present in the passive film in the form of $Mo^{6+(ox)}$. This is in good agreement with Brox and Olefjord's results on the 316 SS (15). In the $Mo3P_{3/2}$-Nls region the Nls signal has been resolved in three nitrogen species N(1), N(2) and N(3). On the basis of previously reported results (13) the peak located at low binding energy (N (1) at 397.7±0.1 eV) is associated to nitride incorporated in the passive film. The peak located at a higher binding energy (N (2) at 400.2±0.1 eV) may originate from N-H or NO (15). The third peak located at an even higher binding energy (N (3) at 402±0.1 eV), may originates from nitrogen in ammonium (16).

Figures 6 and 7 show the spectra of $Cr2p_{3/2}$, Ols, $Mo3d_{5/2,3/2}$ and $Mo3p_{3/2}$-N1s recorded after passivation (30 minutes) of the Fe17Cr13Ni3Mo0.07N alloy in 0.5M H_2SO_4+0.8M NaCl and 1.5M NaCl (pH=1.5) solutions for two take-off angles 90° and 45°. In these agressive solutions the ratios areas of Cr^{3+} hydroxide and oxide (ICr^{3+}(hyd)/ICr^{3+}(ox)) increases with decreasiong take off angle. These results show that the Cr hydroxide, is located in outer part of the passive layer (enhanced signal at 45°). The O1s signal which has a OH^- component partly related to Cr^{3+hyd} shows the same tendency. The major difference between the surface composition in 0.5M H_2SO_4+0.8M NaCl and 1.5M NaCl (pH=1.5) solutions are the following: the signals from Cr^{3+ox} and O^{2-} are enhanced in 1.5M NaCl (pH=1.5) solution. In oposition the N(1), N(2), N(3), Cr and Mo signals are enhanced in 0.5 M H_2SO_4+0.8M NaCl solution, (i. e. the rate of segregation of N, enrichement of Cr and Mo and selective dissolution of iron is higher in 0.5M H_2SO_4+0.8M NaCl solution). These results confirm the idea that nitrogen bonded to chromium (chromium nitride) is formed during the dissolution stage preceding passivation.

In order to investigate the effects of alloy dissolution and potential on the segregation of nitrogen in the passive film a complementary experiment was carried out in 0.5M H_2SO_4+0.8M NaCl solution for the Fe17Cr13Ni3Mo0.07N alloy using the following experimental conditions: the sample was first sumitted to a potentiodynamic sweep from the corrosion potential to 650 mV/SHE (in the passive region); then it was maintained at this potential for 30 minutes Figure 8 shows the spectra of $Cr2p_{3/2}$, Ols, $Mo3d_{5/2,3/2}$ and $Mo3p_{3/2}$-Nls this complementary experiment revealed that N(1), N(2) and N(3) are also mostly formed in this condition.

In order to investigate the effect of nitrogen concentration of the alloy on the chemical composition of the passive film, passivation experiments were carried out for the Fe17Cr13Ni3Mo0.15N in 0.5M H_2SO_4+0.8M NaCl solution at 650 mV/SHE, 30min. Figure 9 shows the spectra of $Cr2p_{3/2}$, Ols, $Mo3d_{5/2,3/2}$ and $Mo3p_{3/2}$-Nls for the take-off angle 90°. Inspection of Mo3p-Nls spectra reveals,three intense N1s signals at the position of N(1), N(2) and N (3). N(1) corresponds clearly to N-metal bonds formed by surface segregation of bulk nitrogen, N(2) and N(3) are thought to originate from nitrogen located at the surface of the film and which has reacted with the electrolyte (i. e. the intensity of N(1) increase with the nitrogen content in the alloy and the intensities of N(2) and N(3) increases with the rate of dissolution and solution charged by nitrogen).

To aid in locating the positions of the different species in the passive film, composition depth profiles were recorded by ion sputtering and XPS analysis for Fe17Cr13Ni0.07N polarized in 0.5M H_2SO_4, 0.5M H_2SO_4+0.8M NaCl and 1.5M NaCl (pH=1.5). The results are shown in fig 10. The XPS signal emitted by O^{2-} in the passive film is shown as an indicator of the depth scale during argon ion sputtering. In both media the OH^-/O^{2-} intensity ratio de-

Ni0.15N alloys in 1.5M NaCl(pH=1.5) solution. The results in fig 4 and the data in table 4 show that i)in the active region the dissolution similar to the variation in 0.5M H_2SO_4+0.8M NaCl solution, ii) the active/passive transition potential (maximum in the i-E curves) is shifted to more anodic potentials with Mo containing alloys iii) the current in the passive state increases with N concentration for the Mo containing alloys, iv) the alloy 0.15N-3Mo pit readily whereas the alloy 0.07 N-3Mo is more resistence to pitting. More breakdown/repassivation events are observed on the high N steel.

2) XPS analysis of the passive films

The spectra of $Cr2p_{3/2}$ Ols $Mo3d_{5/2,3/2}$ and $Mo3p_{3/2}$-Nls recorded after argon ion sputter cleaning and after passivation of the Fe17 Cr13 Ni3 Mo 0.07N alloy in 0.5M H_2SO_4 solution are shown in Fig. 5 for the take-off angle of 90° (angle of the sample surface with the direction in which the electrons are analysed). The observation, for the passivated alloy, of the signals emitted by Cr and Mo (underlying alloy elements) indicates that the passive film is very thin.The chromium signal was resolved by curve fitting into chromium oxide $Cr^{3+(ox)}(Cr_2O_3)$ and chromium hydroxide $Cr^{3+(hyd)}(Cr(OH)_3$ type).

Table 2. Electrochemical data in 0.5M H_2SO_4

Alloys	Corrosion potential (mV/SHE)	Passivation potential (mV/SHE)	Current density maximum ($\mu A/cm^2$)	Residual Current in the passive state ($\mu A/cm^2$)
Fe17Cr13Ni3Mo0.07N	-80	-10	4	2
Fe17Cr13Ni0.15N	-159	-40	1225	2
304 type SS	-130	-70	18	1.8

Table 3. Electrochemical data in 0.5M H_2SO_4 + 0.8M NaCl

Alloys	Corrosion potential (mV/SHE)	Passivation potential (mV/SHE)	Current density maximum ($\mu A/cm^2$)	Residual Current in the passive state ($\mu A/cm^2$)
Fe17Cr13Ni3Mo0.15N	-110	-40	48	1.8
Fe17Cr13Ni3Mo0.07N	-110	-40	19	1.3
Fe17Cr13Ni0.15N	-180	-20	5000	40
316 type SS	-160	-70	400	8

Table 4. Electrochemical data in 1.5M NaCl (pH=1.5)

Alloys	Corrosion potential (mV/SHE)	Passivation potential (mV/SHE)	Current density maximum ($\mu A/cm^2$)	Residual Current in the passive state ($\mu A/cm^2$)
Fe17Cr13Ni3Mo0.15N	-95	0	10	1.4
Fe17Cr13Ni3Mo0.07N	-95	-30	4.2	0.8
Fe17Cr13Ni0.15N	-175	-40	280	25

tion under applied potential, rinsed immediately in ultra-pure water, dried in nitrogen gas and then transferred to the surface analysis system using the transfer vessel and the fast entry port located on the preparation chamber of the spectrometer. A survey XPS spectrum of each sample was immediately recorded to determine its surface cleanliness. The presence of a Cls signal reveals the existence of a contamination layer. The only metallic elements detected were the constituting elements of the alloy. The data processing of high resolution spectra of Fe2p, Cr2p, Ni2P, Ols, Mo3d Mo3p-Nls, S2p and Cl2p allowed us to identify the elements and their chemical states in the passive films. The data processing is based on reference data obtained for the clean and oxidized stainless steels. XPS measurements were obtained using an Al Kα X-ray source (hυ=1486.6 eV), and a hemispherical analyser, with a pass energy of 20 eV for the high resolution spectra.

The spectrometer (VG ESCALAB MK II) was calibrated using the $Au4f_{7/2}$ (binding energy (BE)=84eV) and $Cu2p_{3/2}$ (BE=932.7 eV) peaks. The presence of Mo also complicates the analysis of the N1s XPS spectra due to overlap in binding energy of electrons originating from Nls and $Mo3p_{3/2}$ core levels. To obtain reference spectra, we have synthetized and characterized MoO_2 and MoO_3 with the Al X-ray source. A pure Mo single crystal (111) face) was mounted on a heatable sample holder and cleaned by ion sputtering prior to oxidation. MoO_2 was prepared using the following oxidation conditions: $PO_2=10^{-5}$ mbar, T=600°C, t=40 min. MoO_3 was prepared on the single crystal surface under the following conditions: $PO_2=10^{-1}$ mbar, T=400°C, t=15 min. The spectra are shown in figure 1. The spectra of the figure lb were fitted with two doublets assigned to the species $Mo^{4+(ox)}$ and $Mo^{4+}_{(ox\text{-}hyd)}$ (ox=oxide and hyd=hydroxide) according to the corresponding Ols signals ($O^{2-}$and OH^-). The Mo3d and Mo3p spectra of the passivated alloys could all be fitted with the above chemical states, thus other Mo oxides which have been detected in other works (Mo_2O_3, Mo_2O_5) (14) were not considered here. Composition depth profiles of the passive films on the stainless steels were obtained by ion sputtering the surface, using a VG AG60 ion gun mounted in the analysis chamber, under the following conditions: an ion beam voltage of 4KV an a current density of 0.5μA cm^{-2}.

Results and Discussion

1) Electrochemical behaviour

Figure 2 shows the potentiodynamic (i-E) curves for the Fe17 Cr13 Ni3 Mo0.07N alloy, Fe17 Cr13 Ni0.15N alloy (studied in a previous work (to be published) and the 304 type SS in 0.5 M H_2SO_4 solution. The salient electrochemical features are reported in table 2. The current at the peak maximum varies in the following order: alloy with 0.15% N without Mo>>304 type SS>alloy with 0.07%N and 3% Mo. The major difference is mainly associated with the presence of 3% Mo in Fe17 Cr13 Ni3 Mo0.07N alloy and a small amount of Mo (0.14%) in 304 type-stainless steel. Similar effects have already been observed for Mo implanted Fe-Cr-Ni alloys (6). The residual currents in the passive state are similar for the three alloys.

Figure 3 shows the potentiodynamic curves for the Fe17 Cr13 Ni3 Mo0.15 N, Fe17 Cr13 Ni3 Mo0.07N and Fe17 Cr13 Ni0.15N alloys in 0.5 M H_2SO_4+0.8M NaCl solution.The polarization curve for thye 316-type stainless steel is also included in the figure for comparison. The results in fig 3 and the data in table 3 show that i) in the active region, the dissolution current densities vary in the following order: alloy with 0.15%N without Mo>316 type SS>alloy with 3Mo-0.15N>alloy with 3Mo-0.07N,ii) the alloys without Mo have a small range of passivity. In the passive state, the current increases with increasing N content and decreasing Mo content and iii) there is no detectable pitting with the alloys containing 3%Mo but pitting is observed with 316 type SS and the Alloy without Mo. The resistance to pitting of the 316 is more better then the one of the alloy with 0.15N which does not contain molybdenum.

Figure 4 shows the potentiodynamic curves for the Fe17Cr13Ni3Mo0.15N, Fe17 Cr13 Ni3 Mo0.07N and the Fe17 Cr13

rosion resistance(7-11). However, the development of an understanding of the role of nitrogen in the corrosion behaviour of austenitic stainless steels has been impeded by the fact that the alloys investigated contain significant amounts of molybdenum and, therefore, the observed differences in corrosion from nitrogen-free steels may be due to synergistic effects between molybdenum and nitrogen instead of nitrogen alone. In previous studies (A. Sadough and P. Marcus (12), P. Marcus and M. Bussell. (13) have shown, with XPS and electrochemical measurements, that nitrogen alone (i. e. in the absence of Mo) does not influence on the polarization of the studied alloy (Fe17Cr13Ni0.15N) and nitrogen-implanted autenitic stainless steels in acid solution.

The aim of this work is to investigate, by electrochemical and surface analytical measurements, the effect of nitrogen in the presence of molybdenum on the dissolution and passivation of austenitic stainless steels. XPS and electrochemical measurements have been done on a Fe17 Cr13 Ni3 Mo 0.07 N alloy, to determine the role of Mo and N in the passive film formed in different acidic solutions with and without chloride. We have also compared the electrochemical behaviour of Fe17 Cr13 Ni3 Mo0.07N with the one of other alloys: Fe17 Cr13Ni3Mo0.15N, Fe17Cr13Ni0.15 N, 304-type stainless steel and 316-type stainless steel.

Experimental

The alloy is an austenitic stainless steel (Fe17Cr13Ni3Mo) supplied by IRSID Unieux (France). For the electrochemical study a 304-type stainless steel and three other alloys containing Mo and/or N (Fe17Cr13Ni0.15 N, Fe17 Cr13Ni3Mo0.15 N and a 316-type stainless steel) have been investigated. The elementals composition of the alloys listed in table 1. The alloys were mechanicaly polished with 0.5μm diamond paste, giving them a miror-like finish The electrochemical experiments were carried out in an inert gas glove box. Three different solutions have been used: 0.5M H_2SO_4 (pH=0.4), 0.5M H_2SO_4+0.8M NaCl (pH=0.15) and 1.5M NaCl (adjusted to pH=1.5 with HCl). The electrolyte was deaerated by purging with nitrogen.Sample disks of 10 mm diameter were mounted in the electrochemical glass cell,. equipped with a platinum counter electrode and a mercurous sulfate reference electrode. The electrode potentials reported in this work are referenced to the stanard hydrogen. electrode (SHE). Following insertion of the samples into the electrochemical cell, they were cathodically reduced (-1V, 300s) prior to the measurement of the anodic polarization curve. The polarization curves were recorded using a voltage sweep rate of 1 mV/s while sample passivation prior to surface analysis was carried out by a potential step to 650 mV (SHE) for 30 minutes. The passivated electrodes were removed from solu-

Table 1. Elementals composition of the alloys (wt%)

Alloys	Fe	Cr	Ni	Mo	N	Cu	Mn	Si	C	P	S
Fe17Cr13Ni3Mo0.15N	66.8	17	13	3	0.157	-	-	-	-	-	-
Fe17Cr13Ni3Mo0.07N	66.9	17	13	3	0.07	-	-	-	-	-	-
Fe17Cr13Ni0.15N	69.8	17	13	-	0.157	-	-	-	-	-	-
304-type SS	72.01	17.38	8.28	0.14	0.04	0.15	1.43	0.49	0.05	0.03	0.0025
316-type SS	67.480	17.368	11.025	2.163	0.042	0.151	1.648	0.564	0.025	0.035	0.002

Chemical Composition, Chemical States and Resistance to localized Corrosion of Passive Films on the Nitrogeń and Molybdenum Containing Austenitic Stainless Steels.

A. Sadough-Vanini

Assist. Prof. of Mechanical Eng. Dept.
Amirkabir Univ. of Tech.

Abstract:

Austenitic stainless steels (Fe17Cr-13Ni) with molybdenum (3 wt%) and nitrogen (0.07 wt%) have been characterized by XPS after Passivation. The effects of molybdenum and nitrogen on the passivation of the alloy in 0.5M H_2SO_4, 0.5M H_2SO_4+0.8M NaCl and 1.5M NaCl (PH=1.5) solutions have been investigated. Prior to the electrochemical experiments, the alloy surface was cleaned by argon ion etching in the preparation chamber of the spectrometer. After XPS analysis the samples were transferred without exposure to air into a glove box with an inert atmosphere for electrochemical testing. The electochemical behaviour of the alloy is significantly modified by the molybdenum and nitrogen, as shown by the comparison between Fe17Cr13Ni3Mo0.15N, Fe17Cr13Ni3Mo0.07N, Fe17Cr13Ni0.15N, 316-type stainless steel and 304-type stainless steel. The pitting resistance of the alloys in 1.5 M NaCl was found to be noticably better for the alloy with 3Mo- 0.07N than for the alloy with 3Mo -0.15N.

Surface analysis by XPS of the Mo3p-Nls region and peak fitting shows that after passivation of the alloys three chemical states of nitrogen are present. The low binding energy peak of nitrogen corresponds to nitride which is incorporated in the passive film. The high and intermediate binding energy peaks of nitrogen correspond to nitrogen species located on the surface of the passivated alloys, which are produced by reaction with the solution. The nitrogen spece corresponding to the high binding energy peak is not stable under the X-ray beam.

The passive film was found to have a bilayer structure (inner oxide and outer hydroxide) both in the absence of Cl^- and in the presence of Cl^- in the stage preceding pitting. The outer hydroxide layer contains molybdenum cations in the 6+ chemical state and Mo^{4+} is also detected. In the presence of Cl^-, Cl^- are incorporated in the passive film where they are located mostly in the outer part of the film.

Introduction

The improvement of the corrosion resistance of stainless steels in chloride solution obtained by alloying Mo to austenitic stainless steels is well known, and XPS and electrochemical studies of Mo-containing alloys have been reported (1-6). Nitrogen is always present in stainless steels, usually in small amount as an impurity, but sometimes in more significant amount as an alloying element. Several papers have reported that the addition of nitrogen to austenitic stainless steels increases the cor-